Flow over a glider canopy

A. S. Jonker

J. J. Bosman

School of Mechanical and Nuclear Engineering
North-West University (Potchefstroom campus)
Potchefstroom
South Africa

E. H. Mathews

L. Liebenberg
lliebenberg@researchtoolbox.com

Centre for Research and Continued Engineering Development
North-West University (Pretoria campus)
Lynnwood Ridge
South Africa

ABSTRACT

In order to minimise drag, the front part of most modern glider fuselages is shaped so that laminar flow is preserved to a position close to the wing-to-fuselage junction. Experimental investigations on a full-scale JS1 competition glider however revealed that the laminar boundary layer in fact trips to turbulent flow at the fuselage-to-canopy junction position, increasing drag. This is possibly due to ventilation air leaking from the cockpit to the fuselage surface through the canopy seal, or that the gap is merely too large and therefore trips the boundary layer to turbulent flow. The effect of air leaking from the fuselage-to-canopy gap as well as the size of the gap was thus investigated with the use of computational fluid dynamics. It was found that if air was leaking through this gap the boundary layer would be tripped from laminar to turbulent flow. It was also found that the width of the canopy-to-fuselage gap plays a significant role in the preservation of laminar flow. If the gap is less than 1mm wide, the attached boundary layer is able to negotiate the gap without being tripped to turbulent flow, while if the gap is 3mm and wider, it will be tripped from laminar to turbulent flow. The work shows that aerodynamic drag on a glider can be significantly minimised by completely sealing the fuselage-to-canopy gap and by ensuring a seal gap-width of less than 1mm.

Paper No. 4038. Manuscript received 23 July 2013, revised version received 3 March 2014, accepted 3 March 2014.

https://doi.org/10.1017/S0001924000009428 Published online by Cambridge University Press

NOMENCLATURE

D	drag (N)
h	gap width (mm)
L	lift (N)
(L/D)	glide ratio (–)
P	drag penalty, (N)
R_h	gap width-based Reynolds number (–)
U_∞	free-stream velocity (ms^{-1})
V	airspeed (km/h)
W	weight of glider, (N)
$\Delta Drag$	drag difference between base line and case under consideration, (N)

1.0 INTRODUCTION

The cockpit section of all gliders is designed to house the pilot in the most aerodynamically efficient manner possible[1]. The aim of any cockpit design is to reduce the frontal area of the fuselage while providing the pilot with a comfortable seat and a large canopy to allow good visibility[2]. The large canopy found on most modern gliders however facilitates efficient solar heating of the cockpit, especially on cloudless days. For thermal comfort of the pilot, this excess heat should be extracted by a ventilation system.

A number of problems are, however, associated with such ventilation. First, the ventilation air adds to the total aerodynamic drag of the glider. This is due to the flow resistance through the internal ducts that channel the flow from the glider-nose air inlet to the various areas in the cockpit. The internal drag can be reduced by providing ducting with a large enough diameter so that the internal flow velocity will be low[3].

The second problem is that ventilation air that enters a glider cockpit must be properly expelled from the aircraft to prevent any adverse effects on the performance. If the velocity of the air leaving the glider is less than the outside air speed at the outlets, then the drag increase due to momentum change would be significant[4]. Also if the expelled air separates from the aircraft skin, an additional drag penalty will result[5].

Separation problems can be minimised by allowing the air to exit at the very rear end of the fuselage, as is current practice on most gliders. The location of the air outlet at the rear of the glider together with several narrow channels and bulkheads through which the air is ducted in the aft fuselage, result in increased internal flow resistance. The blockage is often so severe that the ventilation air flow rate is so low that many pilots complain that present systems do not provide sufficient ventilation in extreme ambient conditions[6].

The third problem follows from the second. If the flow resistance of the air outlet and ducting is too large, a positive pressure will result in the glider fuselage. This, in turn, forces air to leak from any location where the fuselage is not properly sealed[7,8]. Several of the older generation of gliders do not have any escape route for the ventilation air and air will leak out of any opening. The leaking air usually causes the boundary layer on the outside of the glider to separate, or to trip the laminar flow regions to turbulent flow, with an associated skin friction drag penalty and loss of performance[5].

Problem areas, where leaking air is common, are the fuselage canopy seal and the wing-to-fuselage interface. If the wing/fuselage interface is airtight, the leaking air can find its way down the wing and out the airbrake box or flapperon drivers. The wings of most gliders are, however, sealed with rubber seals around the control system tubes so that the leaking air cannot enter the wing.

https://doi.org/10.1017/S0001924000009428 Published online by Cambridge University Press

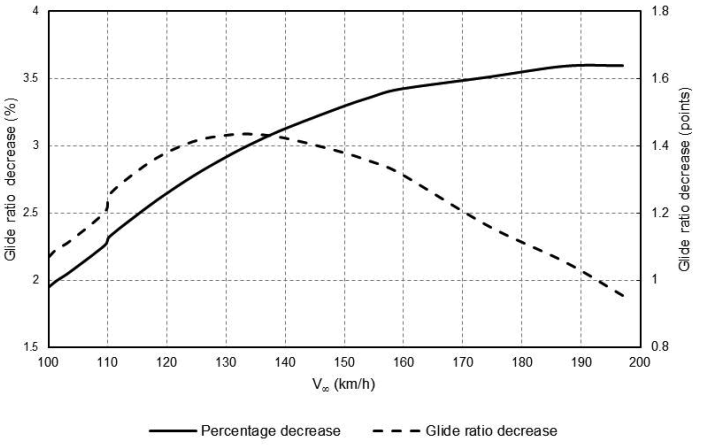


Figure 1. Performance decrease when the boundary layer over the canopy of a JS1 competition glider is turbulent instead of laminar.

It is difficult to ensure an airtight seal between the fuselage and the canopy due to manufacturing constraints. This results in some air leaking through this interface area if the fuselage is under positive pressure. If air is leaking on the front edge between the canopy and fuselage, the laminar boundary layer at this point will be tripped to turbulent flow.

Holmes *et al*[9] have shown that if there is no leaking through a gap, then laminar boundary layer will not be tripped to turbulent flow, but only if the gap is narrow enough. The flow will remain laminar over the gap if the Reynolds number, $R_h = (U_\infty/\nu)h$, based on the free stream airspeed U_∞ and the kinematic viscosity ν, and length of the gap h, is smaller than 15,000.

Figure 1 illustrates the typical performance decrease when the boundary layer over the canopy of a JS1 competition glider is turbulent instead of laminar. The data for the graphs were calculated from flat plate skin friction factors[10] and adapted to the geometry and performance of the JS1 glider. The total wetted surface area of the canopy was approximated as one square meter.

The largest calculated performance decrease is at high speed with a 3·5% performance reduction. At low-speed the performance loss is approximately 1·9%. This is a performance loss of 1 lift-to-drag ratio point at high-speed and 1·4 lift-to-drag ratio points at low speed.

It is seen from the data that the state of the boundary layer on the canopy has a significant effect on performance. The fuselage-to-canopy gap influences the development of the boundary layer on the front part of the cockpit. The purpose of this research was thus to numerically investigate the effect of the fuselage-to-canopy interface gap size and the influence of leaking air on the flow condition over the canopy. The JS1 prototype competition glider was used as test platform for this investigation.

2.0 FUSELAGE BOUNDARY-LAYER CHARACTERISTICS

The shape of the JS1 glider fuselage was optimised to ensure laminar flow over the largest possible area in order to minimise drag. This was achieved by deriving the front fuselage shape from that of a laminar aerofoil. The two-dimensional aerofoil shape was transformed into a three-dimensional shape by applying the method of Galvao[11]. Figure 2 shows the pressure distribution over the front part of the fuselage along its centreline as calculated with the panel code KK-Aero[12]. The pressure decreases to the widest part of the fuselage and laminar flow is therefore theoretically possible to a point close to the wing-fuselage interface[13].

https://doi.org/10.1017/S0001924000009428 Published online by Cambridge University Press

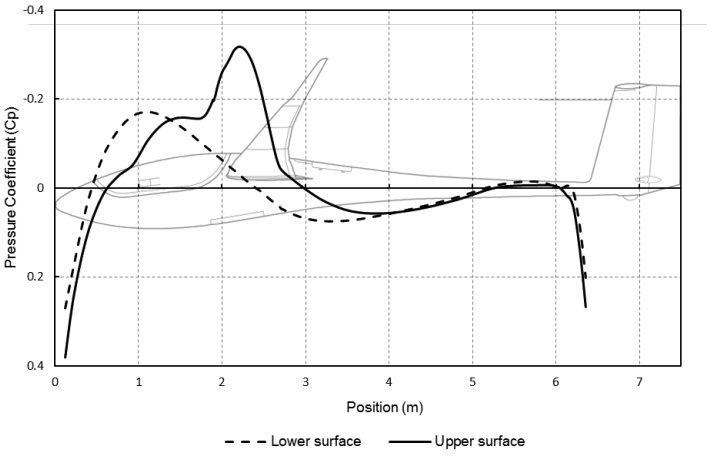


Figure 2. Pressure distribution on fuselage top and bottom surfaces calculated with the panel code KK-Aero(12), superimposed with line diagram of the JSI fuselage profile.

The canopy gap on the JS1 glider is typically 2·5mm wide which gives a $Re_h = 5{,}341$, i.e. < 15,000. The laminar flow regime should therefore not be tripped to turbulent flow by the canopy gap. Unfortunately, much less laminar flow is present on the front part of the glider, as was revealed during flight test measurements.

The laminar flow region on the front part of the fuselage was determined in-flight on the JS1 glider by the acoustic measurement technique as described by Schumann[5]. A thin pipe was connected to a stethoscope; the free end of the tube was positioned in the flow field where the boundary-layer condition had to be determined. A soft whistling sound indicated laminar flow and a loud rumble was indicative of turbulent flow. It was found during wind-tunnel testing that the probe tripped the laminar boundary layer to turbulent flow at the test position. This transition, however, occurred downstream of the probe and did not influence the sound that was detected.

During the test flying, the probe was positioned on the outside of the fuselage at various positions while the boundary-layer condition was mapped, as shown in Figs 3 and 4. The measurements were taken at indicated airspeeds between 100km/h and 150km/h during calm atmospheric conditions, while the probe was placed into the free stream through the storm window. It was possible to measure the transition point with an accuracy of ± 5mm over the length of the canopy which is approximately 1,500mm long. This resulted in a canopy drag measurement error of ± 2·5% and an overall drag error of ± 0·01%.

It was found that the laminar boundary layer does not extend past the canopy forward edge and that the flow on most of the canopy was turbulent. This is probably due to the canopy edge that trips the laminar boundary layer to turbulent flow. The canopy-to-fuselage gap was approximately 2·5mm wide and the test airspeed was 120km/h. The flow on the sides of the fuselage below the canopy was found to extend to a position 1,500mm from the nose of the glider. It was not possible to measure the condition of the boundary layer on the bottom side of the fuselage using this method.

The in-flight testing showed that the canopy edge disturbed the boundary layer enough so that the boundary layer is tripped from laminar to turbulent flow. This prevents the fuselage from achieving the theoretically predicted laminar flow and concomitant low drag. In order to better understand this phenomenon, it was decided to conduct a computational fluid dynamics (CFD) investigation on the effect of the canopy-to-fuselage gap on the boundary layer.

https://doi.org/10.1017/S0001924000009428 Published online by Cambridge University Press



Figure 3. Measurement method for acoustic mapping of the boundary layer of the JS1.



Figure 4. Acoustic mapping on the JS1 canopy boundary layer during flight.

3.0 CFD ANALYSIS

3.1 CFD set-up

For the CFD simulation, the fuselage of the JS1 without the wings and empennage was modeled for simplicity. The computational flow domain is illustrated in Fig. 5. Only half of the fuselage was simulated where a symmetry plane was used in order to reduce the sise of the mesh and thus the computational requirements. An internal interface ring was placed around the fuselage which facilitated easy angle-of-attack changes during the meshing phase.

The tetrahedral meshes which included boundary-layer prism cells were constructed using STAR CCM+® (Fig. 6) which allows for high-quality automatic meshing. The meshes were then exported to ANSYS Fluent® where the three-equation eddy-viscosity RANS flow model by Walters and Leylek[14] was applied and solved. The transition model does not use intermittency transport equations but rather transport equations for turbulent kinetic energy, laminar kinetic energy and the inverse turbulent time scale which provides a more accurate description of the stream-wise fluctuations occurring in boundary layers. The standard transition model constants were used.

The analysis was performed on a high-performance computer cluster with 80 gigabytes of memory and 28 parallel processors. The simulations typically contained 30 million cells and the average runtime to convergence was 12 hours.

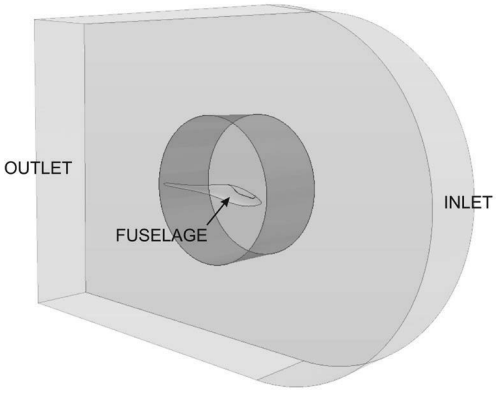


Figure 5. Flow domain used for the canopy flow test cases.

https://doi.org/10.1017/S0001924000009428 Published online by Cambridge University Press

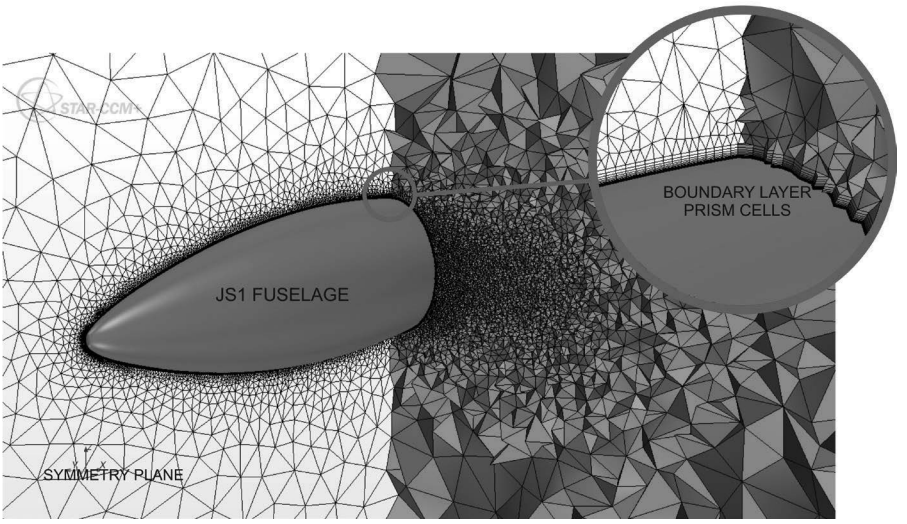


Figure 6. Tetrahedral mesh with prism boundary-layer cells around the fuselage.

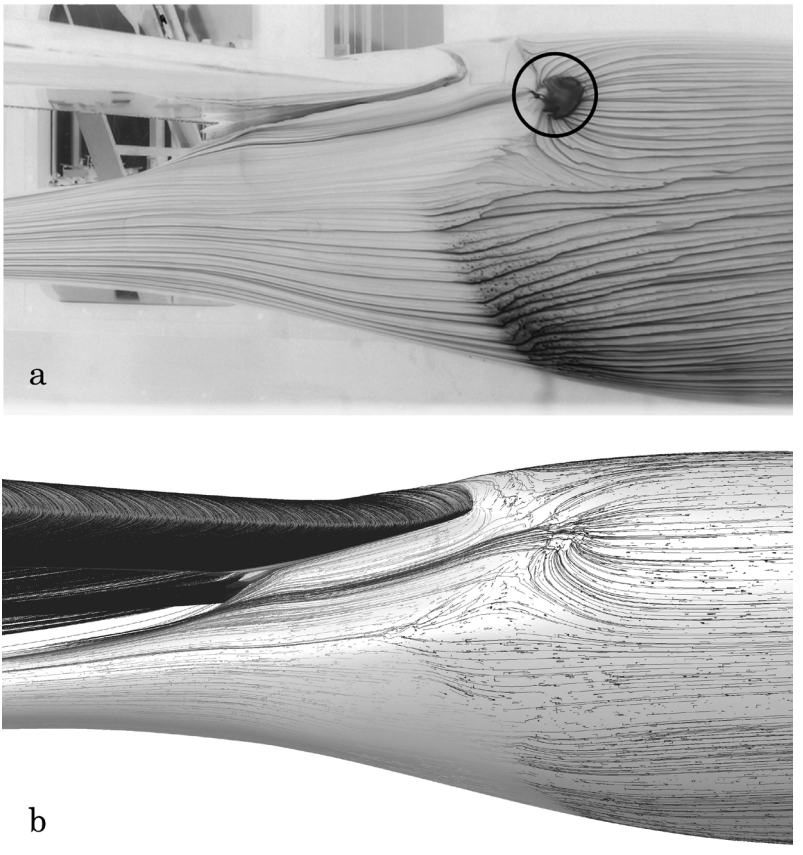


Figure 7. Oil flow visualisation showing transition positions on the Mü31 model (Reynolds number, Re = 1·5 × 10^6, V_∞ = 303km/h, 0° flap setting).

https://doi.org/10.1017/S0001924000009428 Published online by Cambridge University Press

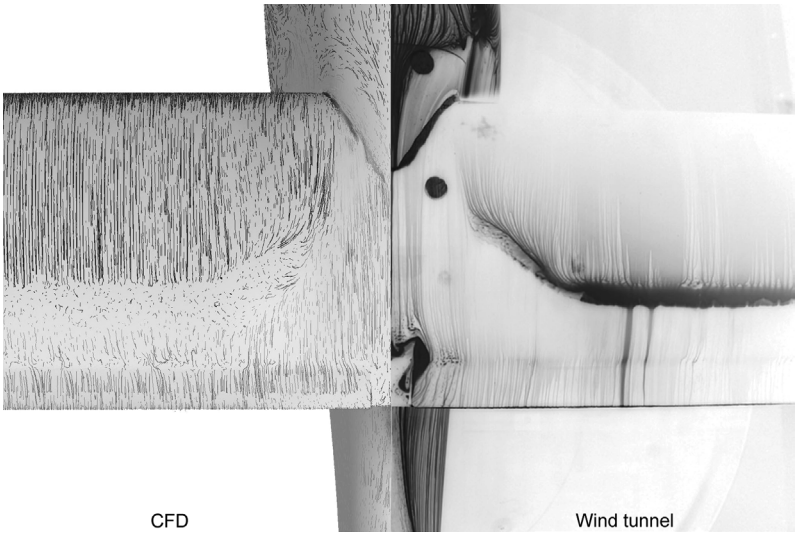


Figure 8. Oil flow results from the wind-tunnel experiments in comparison with the CFD results (Re = 1·5 × 10^6, V_∞ = 303km/h, 0° flap setting).

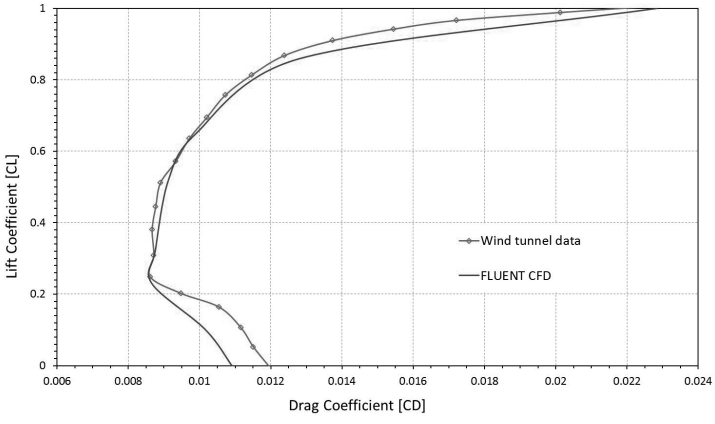


Figure 9. Polar plot for the 1:3 scale Mü31 model (Re = 1·5 × 10^6, 0° flap setting), showing wind-tunnel data versus CFD-predicted data.

The computational mesh resolution has a large effect on the drag estimation of components. All simulations were therefore conducted with adequate mesh resolution so that the drag values obtained were independent of the small mesh variations between the different simulations. The prediction of the transition location is, however, less influenced by the resolution of the mesh, although the minimum y^+ values ($y^+ < 1$) were obtained as specified by the transition model.

3.2 CFD data validation

The CFD data were validated using wind-tunnel data from the low- speed laboratory of the Technical University in Delft. Lift and drag measurements as well as oil flow visualisations for various configurations of the 1:3 scale model Mü31 glider (with a similar front fuselage to the JS1 glider) were compared against CFD results. Figures 7 and 8 show oil flow visualisations of the wind-tunnel

https://doi.org/10.1017/S0001924000009428 Published online by Cambridge University Press

experiments and CFD simulations. The results show that the CFD-predicted laminar-to-turbulent transition model is adequate for predicting the location of transition. When comparing the drag and lift values (Fig. 9) it can also be seen that the CFD model accurately captures the low drag 'bucket'. This implies that the overall boundary-layer phenomena are predicted with sufficient accuracy in order to obtain the appropriate lift and drag values in comparison to the wind-tunnel data.

3.3 Analysis matrix

The numerical investigation was performed at conditions that are close to the typical flight conditions of gliders. The JS1 is an 18m-class competition glider and typical flight speeds vary between 120km/h during the climbing phase and 200km/h during inter-thermal cruising flight. The CFD analyses were therefore performed at two typical flow velocities, 35ms^{-1} (126km/h) and 55ms^{-1} (198km/h).

The effect of the width of the canopy-to-fuselage interface gap as well as the effect of inflow and outflow through the gap were simulated. The analyses were performed with realistic gap widths of 1mm and 3mm, respectively. The canopy circumference of the JS1 is 4,000mm. This gives gap areas of 4,000mm^2 and 12,000mm^2 respectively.

The cockpit nose inlet area is 962mm^2. At 35ms^{-1} the theoretical mass flow into the cockpit is therefore 0·041kg/s, and 0·065kg/s at 55ms^{-1}. As many glider of the older generation do not have any ventilation exit openings and that of newer generation gliders are severely restricted, it was decided to use 0·04kg/s as the maximum possible mass flow that will escape through the canopy gap. For the inflow calculation half of this value (0·02kg/s) was arbitrarily chosen. The analysis matrix is shown in Table 1.

Table 1
Analysis matrix

Case no	Flow velocity (ms^{-1})	Gap dimension (mm)	Flow through gap (kg/s)	Reh
1	35	1	0·00	2,243
2	35	1	0·04	2,243
3	35	3	0·00	6,730
4	35	3	–0·04	6,730
5	55	1	0·00	3,505
6	55	1	0·04	3,505

4.0 RESULTS

4.1 Results for V = 35ms^{-1} (126km/h)

Figure 10 shows the results for Case 1 at V = 35ms^{-1} (126km/h) with a 1mm gap and without any outflow. It can be seen that the flow is able to negotiate the 1mm gap without any difficulties which is in agreement with Holmes[9] as Re_h = 2,243, i.e. < 15,000. The boundary layer remains laminar up to the rear edge of the canopy. This corresponds with the theoretical prediction of a smooth surface without any gaps. Figure 11 shows that there is some circular flow in the gap, but the flow velocity is low enough so as not to affect boundary layer transitioning.

https://doi.org/10.1017/S0001924000009428 Published online by Cambridge University Press

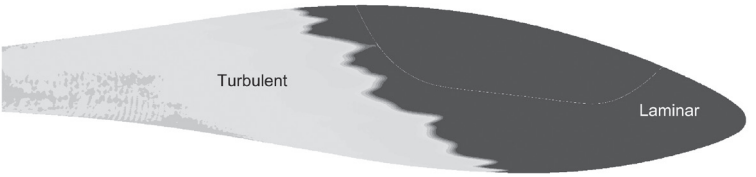


Figure 10. Case 1, turbulent intensity plot (1mm gap, V_∞ = 35ms^{-1} or 126km/h, no blowing).

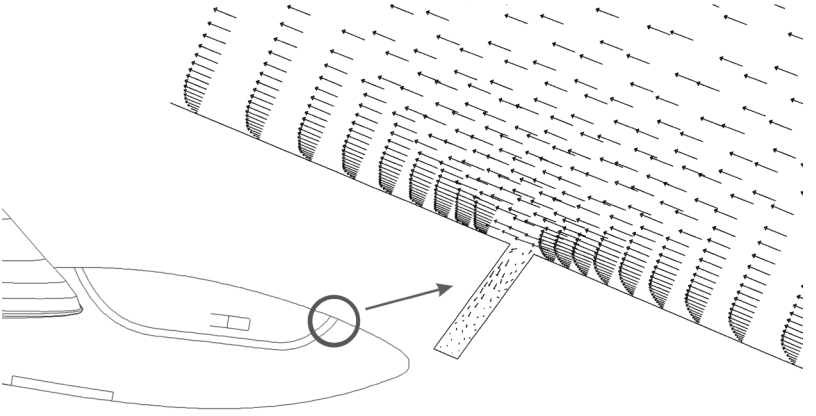


Figure 11. Case 1, velocity vector plot for the case of no forced flow from the gap. (1mm gap, V_∞ = 35ms^{-1}, no blowing).

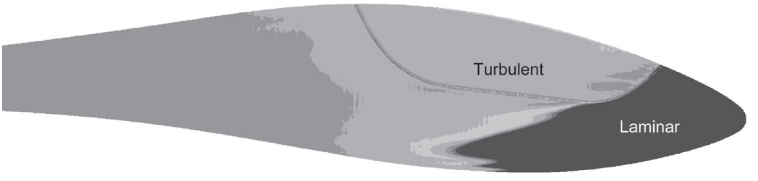


Figure 12. Case 2, turbulent intensity plot (1mm gap, V_∞ = 35ms^{-1}, $\dot{m}$ = 0·04kg/s).

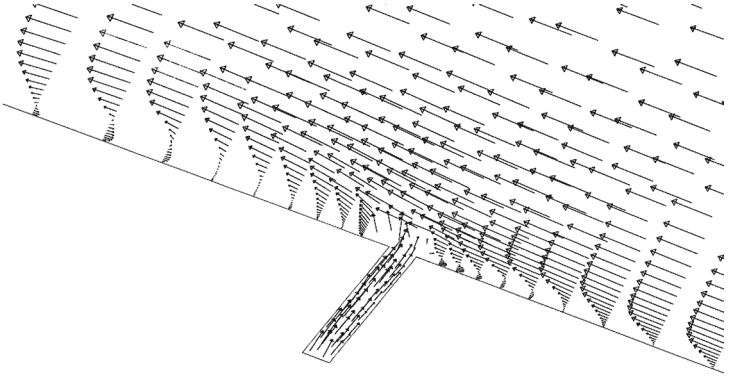


Figure 13. Case 2, velocity vector plot for the case of forced flow in the gap. (1mm gap, V_∞ = 35ms^{-1}, $\dot{m}$ = 0·04kg/s).

https://doi.org/10.1017/S0001924000009428 Published online by Cambridge University Press



Figure 14. Case 3, turbulent intensity plot . (3mm gap, V_∞ = 35ms^{-1}, no blowing).

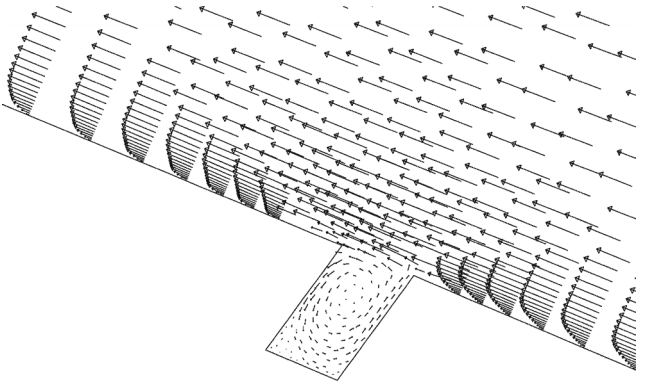


Figure 15. Case 3, velocity vector plot in the case of flow in the gap. (3mm gap, V_∞ = 35ms^{-1}, no blowing).

One may now interrogate whether air outflow from this gap would trip the boundary layer to turbulent flow. Figure 12, Case 2, shows that with 0·04kg/s outflow, the canopy gap indeed trips the boundary layer to turbulent flow. The mass flow is distributed around the whole canopy edge and results in an outflow velocity of between 15 and 25ms^{-1}, as shown in Fig. 13. The outflowing airstream creates a virtual obstacle in the lower level of the boundary layer which slows the flow down to create a small area of reverse-flow upstream of the gap. This also results in a transitioned turbulent boundary layer downstream of the gap. The results in Case 2 are similar to those of the flight test shown in Fig. 4.

Figure 14 shows the flow for Case 3 at 35ms^{-1} with a 3mm wide gap and no forced flow through the gap. It follows that the presence of the 3mm gap trips the boundary layer from laminar to turbulent flow. This result is in contrast with the prediction of Holmes as Re_h = 6,730, < 15,000, and the laminar boundary layer should not have been tripped to turbulent flow.

Figure 15 shows that there is circulation inside the gap which creates vertical flow components at the leading edge of the gap which is sufficient to trip the boundary layer from laminar to turbulent flow.

It was then determined whether the boundary layer at this position could be stabilised by applying suction through the gap. Figure 16 shows the case with realistically achievable

0·02kg/s suction applied through the gap. This indeed stabilises the flow so that the full extent of the laminar flow potential can be reached. It follows that the flow is now again laminar to a point behind the rear edge of the canopy.

4.2 Results for V = 55ms^{-1} (198km/h)

The next set of result is for the high-speed case of V = 55ms^{-1} (198km/h). Figure 17 shows that laminar flow also extends past the 1mm gap at high speed but that the flow is less stable.

https://doi.org/10.1017/S0001924000009428 Published online by Cambridge University Press

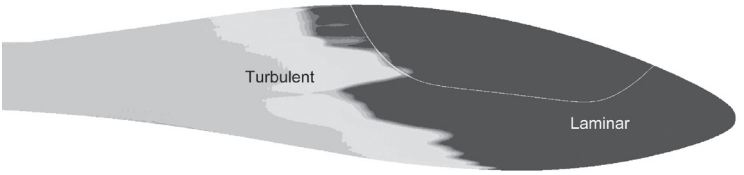


Figure 16. Case 4, turbulent intensity plot (3mm gap, V_∞ = 35ms^{-1}, $\dot{m}$ = 0·02kg/s suction).

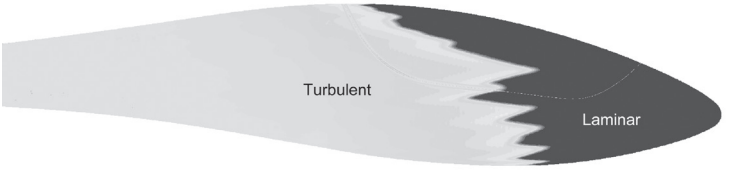


Figure 17. Case 5, turbulent intensity plot (1mm gap, V_∞ = 55ms^{-1}, no blowing).

Also, the transition point is further upstream than for the low-speed case, as predicted by the higher Reynolds number. The velocity of the circular flow in the gap is still low enough not to influence the boundary layer crossing the gap. This is also in agreement with Holmes[9] as Re_h = 3,205, < 15,000.

At 55ms^{-1} (198km/h) the effect of the outflow is similar to that of the low-speed case in that the boundary layer is tripped to turbulent flow as is shown in Fig. 19.

4.3 Drag data

The total drag for each of the load cases was calculated by integrating the normal and tangential force components over the fuselage body using the Fluent® CFD code. The difference in drag between each test case and a baseline configuration gives the relative performance influence of the test case. For the baseline case the boundary layer is laminar up to the rear edge of the canopy. The drag calculated for each case is summarised in Table 2.

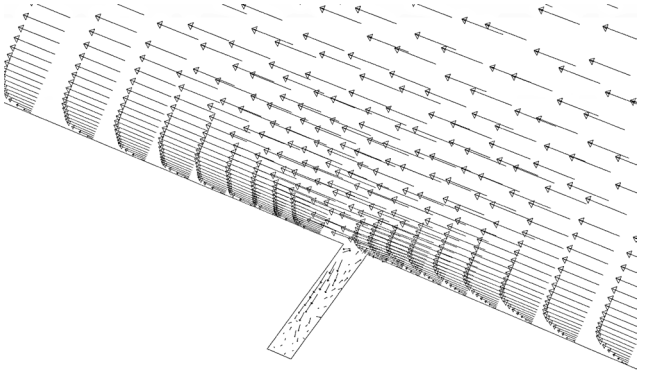


Figure 18. Case 5, velocity vector plot in the case of no forced flow in the gap. (1mm gap, V_∞ = 55ms^{-1}, no blowing).

https://doi.org/10.1017/S0001924000009428 Published online by Cambridge University Press

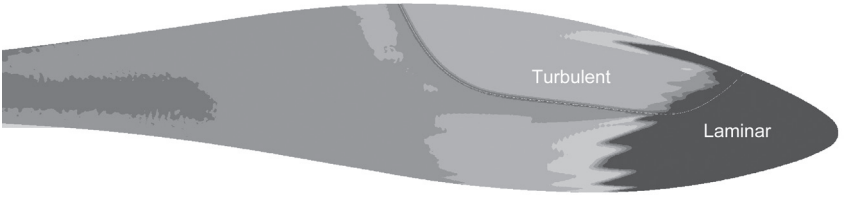


Figure 19. Case 6, turbulent intensity plot . (1mm gap, V_∞ = 55ms^{-1}, $\dot{m}$ = 0·04kg/s).

Table 2
Calculated total drag for each load case

No. velocity (ms^{-1})	Flow dimension (mm)	Gap gap (kg/s)	Flow through drag (N)	Total
1	35	1	0	13·8
2	35	1	0·04	17·7
3	35	3	0	18·2
4	35	3	–0·02	14·6
5	55	1	0	40·0
6	55	1	0·4	43·1

The drag penalty for each case is shown in Table 3. The JS1's theoretical maximum lift-to-drag ratio **(***L/D***)** of 53 at 35ms^{-1} (126km/h), and L/D = 32 at 55ms^{-1} (198km/h), were used to calculate the performance penalty. The maximum laminar flow results of Cases 1 and 5 were used as the baseline configuration at 35ms^{-1} and 55ms^{-1}, respectively. The new lift to drag ratio for the drag increase for each case was calculated using the following equation:

$$\left(\frac{L}{D}\right)_{new} = \left[\left(\frac{L}{D}\right)^{-1}_{baseline} + \frac{\Delta Drag}{W}\right]^{-1} \quad \ldots (1)$$

The difference in drag between the baseline cases 1 and 2 is 13·8N – 17·7N = 3·9N. The new lift-to-drag ratio when the glider mass is 600kg can be calculated using Equation (1) as 51·2, which is a difference of 3·3% from the 53 points of the baseline case.

Table 3 shows that the drag penalty when the boundary layer over the canopy is fully turbulent (Cases 2 and 3), is 3·3% and 3·8% at 600kg glider mass. If boundary-layer suction is applied to the 3mm gap the penalty can be reduced to 0·7% and 0·9% at the respective flying masses. At high speed the penalty is 1·5% at 600kg and 2·2% at 450kg glider mass. This shows that the canopy edge does indeed have a large effect on the overall performance of a modern glider.

5.0 CONCLUSION

It was found that the canopy-to-fuselage interface can have a significant adverse effect on the condition of the boundary layer over the canopy of a modern glider. Results from in-flight measured data compared well with numerical data. A gap of 1mm wide does not seem to affect the boundary

https://doi.org/10.1017/S0001924000009428 Published online by Cambridge University Press

Table 3
Performance penalty for each load case compared to the maximum laminar flow case

Case no [N]	Drag difference	Baseline *L/D*	Performance penalty @ 600kg New *L/D*	(%)	Performance penalty @ 450kg New *L/D*	(%)
2	3·9	53	51·2	3·3	50·6	4·4
3	4·4	53	51	3·8	50·3	5·1
4	0·8	53	52·6	0·7	52·5	0·9
6	3·1	32	31·5	1·5	31·3	2·2

layer if there is no outflow through the gap. Outflow trips the laminar boundary layer to turbulent flow with an accompanying drag penalty of around 4%.

A canopy edge gap of 3mm will trip the flow from laminar to turbulent even if there is no outflow at the gap, with a drag penalty of around 4%. If boundary-layer suction is applied at this gap the flow can be kept laminar. The drag penalty is then only in the order of 0·7%.

At high speed the drag effects are the same for a 1mm and 3mm gap with the laminar flow regions shorter due to the higher Reynolds number. To minimise aerodynamic drag, it is therefore essential to ensure that the fuselage-to-canopy gap is completely sealed and that the gap has a width of less than 1mm.

It was also found that the widely used gap-based Reynolds number Reh-criterium, i.e. $Re_h < 15{,}000$, does not predict the laminar-to-turbulent transition accurately on a curved glider fuselage shape.

REFERENCES

1. ALTHAUS, D. Wind-tunnel measurements on bodies and wing-body combinations, Motorless Flight Research, NASA CR-2315, November 1972.
2. OSTROWSKI, J., LITWINCZYK, M. and TURKOWSKI, L. Characteristics of flow past fuselages and wing-fuselage systems of glider, NASA TM-75401, Washington, DC, USA, National Aeronautics and Space Administration, 1978.
3. SCHREUR, W.B. The ventilation of streamlined human powered vehicles, Human Power eJournal, [online] Available at: <http://www.hupi.org/HPeJ/Index.htm> (Accessed on 18 February 2011), 2004.
4. TAMAI, G. *The Leading Edge: Aerodynamic design of ultra-streamlined land vehicles*, Cambridge, Robert Bentley Publishers, 1999.
5. SCHUMANN, W.E. Glider performance improvements, [online] Available at < http://www.betsybyars.com/guy/soaring_symposia/> [Accessed on 8 October 2012] The 1972 American Soaring Symposium, Mont Chateau Lodge, Morgantown, West Virginia, USA, 12-13 February 1972.
6. SINCLAIR, J.J. Internet forum on glider cockpit ventilation, [online] Available at: <http:// www.aviationkb.com/Uwe/Forum.aspx/soaring/602/ASW-24-27-rear-fuselarge-vents.> [Accessed on 10 December 2010], 2003.
7. BICKLE, P.F. Sailplane Preparation for Competition, Available at: < http://www.betsybyars.com/guy/soaring_symposia/> [Accessed on 8 October 2012], The 1971 American Soaring Symposium, Mont Chateau Lodge, Morgantown, West Virginia, USA, 13-14 February 1971.
8. BOERMANS, L.M.M. and TERLETH, D.C. Wind–tunnel tests of eight sailplane wing-fuselage combinations, *Tech Soaring*, 1983, **8**, (3), pp 70-85.
9. HOLMES, B.J., OBARA, C.J., MARTIN, G.L., GLENN, L. and DOMACK, C.S. Manufacturing tolerances for natural laminar flow airframe surfaces. SAE Paper 850863.
10. SCHLICHTING, H. *Boundary Layer theory*, New York, USA, McGraw-Hill Book Company, 1979.
11. GALVAO, F.L. A note on low drag bodies, OSTIV Publication X, Hobbs: Soaring Society of America, 1968.

https://doi.org/10.1017/S0001924000009428 Published online by Cambridge University Press

12. KUBRYNSKI, K. Application of the panel method to subsonic aerodynamic design; Application of the panel method to subsonic aerodynamic design, *Inv Probl Engng*, 1997, **5**, (2), pp 87-112.
13. GOLDSCHMIED, F. Fuselage self-propulsion by static- pressure thrust – Wind-tunnel verification, AIAA/AHS/ASEE Aircraft Design, Systems and Operations Meeting, 14-16 September 1987, St Louis, Missouri, USA.
14. WALTERS, D.K. and LEYLEK, J.H. Computational fluid dynamics study of wake-induced transition on a compressor-like flat plate, *J Turbomach*, 2005, **127**, (1), pp 52-63.

https://doi.org/10.1017/S0001924000009428 Published online by Cambridge University Press